AUTOMATED MULTI-MODALITY REGISTRATION OF 64-SLICE CORONARY CT ANGIOGRAPHY WITH MYOCARDIAL PERFUSION SPECT

Jonghye Woo[1,2], *Piotr J. Slomka*[2], *Damini Dey*[2], *Victor Cheng*[2], *Amit Ramesh*[2], *Byung-Woo Hong*[3], *Daniel S. Berman*[2], *C.-C. Jay Kuo*[1], *Guido Germano*[2]

[1]University of Southern California, Los Angeles, CA 90089-2564, USA
[2]Cedars-Sinai Medical Center, Los Angeles, CA 90048, USA
[3]Chung-Ang University, Seoul, Korea

ABSTRACT

A multi-modality image registration algorithm for the alignment of myocardial perfusion SPECT (MPS) and coronary computed tomography angiography (CTA) scans is presented in this work. Coronary CTA and MPS provides clinically complementary information in the diagnosis of coronary artery disease. An automated registration algorithm is proposed utilizing segmentation results of MPS volumes, where regions of myocardium and blood pools are extracted and used as an anatomical mask. Using a variational framework, we adopt an energy functional with a piecewise constant image model and optimize it numerically with a gradient descent algorithm. The computational efficiency and robustness of the proposed automatic registration of CTA with MPS have been demonstrated by the experiments that yielded an average error smaller than a MPS voxel size.

Index Terms— multi-modality image registration, image registration, myocardial perfusion SPECT, coronary CTA, variational framework

1. INTRODUCTION

Both coronary computed tomography angiography (CTA) and myocardial perfusion SPECT (MPS) can be used to diagnose coronary artery disease. Coronary CTA allows precise localization of coronary artery plaques and depiction of coronary anatomy [1]. Coronary lesions are responsible for hypoperfusion of myocardium. Myocardial MPS is a mainstream imaging technique used to estimate hypoperfusion in the myocardium caused by coronary lesions, which however cannot be observed by MPS directly. Thus, it is requested to combine different imaging modalities that provide clinically complementary information in the diagnosis and this can be achieved by registration.

In general, registration algorithms can be categorized as "feature-based" and "intensity-based" methods depending on the characteristic information that is used in the computation of dissimilarity measure. Feature-based methods are performed based on local image features such as edges or relevant anatomical structures, whereas "intensity-based" methods directly use image intensity that does not require any additional function for characterizing structures in image. A number of different measures have been applied for the computation of dissimilarity and mutual information is one of the most popular approaches specially for multi-modality image registration [2, 3]. However, in multi-modality registration problems, intensity alone is often insufficient and additional prior knowledge is desired to be incorporated. This is especially true for images from abnormal subjects that have inherent physiological variations between different modalities. In such circumstances, image segmentation can be of great use for registration incorporating the hybrid information such as the boundaries and the intensity distribution in the regions of interest [4].

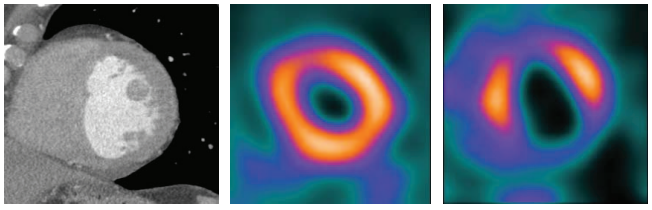

(a) (b) (c)

Fig. 1. Examples of mid-myocardial short-axis images from CTA and MPS: (a) a CTA image which looks similar for normal and abnormal arteries, (b) a normal MPS image and (c) an abnormal MPS image.

In this work, we aim to develop a fully automated multi-modality image registration technique for aligning functional MPS with anatomical coronary CTA scans. To provide robust registration results, we utilize the segmented MPS volume and estimate intensity values in the myocardial and blood pool region simultaneously with a variational framework. The rest of this paper is organized as follows. Previous work is reviewed in Sec. 2. The proposed registration method with segmented MPS volume and its minimization is described in Sec. 3 followed by experimental results presented in Sec. 4.

Finally, discussion and concluding remarks are given in Sec. 5.

2. REVIEW OF PREVIOUS WORK

Visual analysis of fused MPS and coronary CTA images can synergistically improve the diagnostic value of sequential combined imaging [5], and manual tools for CTA-MPS fusion have been developed [6]. However, manual alignment is tedious and observer-dependent, which complicates clinical protocols and reduces the practicality of such tools. The difficulty in accurate registration of MPS with coronary CTA lies in the fact that different anatomical features are visible in different images. For example, the CTA image is created by the attenuation of external photons throughout the thoracic volume while MPS is created by emissions of photons located primarily in the myocardium. Furthermore, although myocardium is visible from both CTA and MPS, there could be severe perfusion defects present on MPS images which do not have equivalent appearance on CTA as shown in Fig. 1. In addition, variations in the intravenous contrast distribution for different patients cause intensity variations on CTA images within the blood pool region. As a result, standard automated registration procedures, such as mutual information without specialized pre-processing may not be most effective.

To the best of our knowledge, a fully automated multi-modality image registration of MPS with coronary CTA scans obtained from stand-alone systems has not been developed previously. Previous studies on fusion between MPS and coronary CTA required laborious manual alignment of image data [5, 6]. Several studies on the registration of MPS with other modalities were conducted. Faber *et al.* [7] proposed a point-based registration of the MPS surface with 3D coronary anatomy reconstructed from invasive 2D coronary angiography. Guetter *et al.* [8] developed a registration method for MPS and non-contrast CT data to improve the attenuation correction. In their studies, images were however obtained by the hybrid SPECT-CT scanner (in contrast with different stand-alone scanners) where images are already in approximate alignment, requiring only small correction. Guetter *et al.* [8] proposed a learning-based method based on the mutual information and an intensity co-occurrence prior. However, this approach used an off-line training process that is computationally inefficient. Besides, all data sets have to be provided a priori; otherwise, the prior model may not be incrementally extended as new image data (*e.g.* different vendors or abnormal data) are available. In related development, Aladl *et al.* [9] proposed an MRI-MPS volume registration technique which utilized the MRI motion to pre-segment the heart for registration with MPS. However, this approach is not practical for CTA since typically only one phase is reconstructed and available for analysis while the use of all frames is computationally intractable.

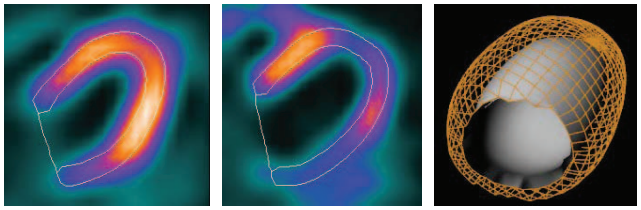

(a) (b) (c)

Fig. 2. An example of myocardial segmentation (white contours) from MPS: (a) the 2D slice of segmented normal MPS, (b) abnormal segmented MPS, and (c) the 3D segmented MPS volume with endocardial boundary (gray) and epicardium boundary (orange mesh).

3. DESCRIPTION OF PROPOSED METHOD

3.1. Pre-processing

In our registration method, a fully automatic segmentation algorithm [10] for the left ventricle (LV) with additional segmentation of the blood pool regions is first adopted to extract structures of interest, including myocardium and the blood pool, in the MPS volume. Segmentation of MPS volumes is of great importance since it can provide the anatomical information to guide registration. Those regions to be extracted from MPS volumes usually do not present distinguished boundary features due to severe perfusion defects, resulting in an inhomogeneous intensity distribution despite within the same anatomical region as shown in Fig. 2.

Let I and J be segmented MPS and coronary CTA volumes, respectively, in Ω, which correspond to an open and bounded domain in $\mathbb{R}^3$. The segmented MPS volume, I, is the union of three disjoint regions; namely, the blood pool, myocardium, and extracardiac structures. We denote regions of blood pool, myocardium, and extracardiac structures by D_1, D_2, and D_3 respectively, and $\Omega = D_1 \cup D_2 \cup D_3$.

Besides the segmentation procedure, it is necessary to match cardiac phases between these two modalities. To achieve this goal, we perform the alignment of coronary CTA with end-diastolic (ED) images as selected for coronary artery analysis with segmented "motion-frozen" MPS created from gated images [11]. In the motion-frozen technique, derived LV contours are used in combination with a thin-plate spline image warping [12] to create the MPS volume in end-distolic phase matching with CTA. For both CTA and MPS, transverse image orientation is used during the registration process.

3.2. Registration Model Using Segmented MPS Volume

The goal of registration is to find the transformation, $T(x)$, that maps the source volume into the corresponding target volume. In this application, we consider 3D rigid registration with 6 parameters (3 for the translation and 3 for the rotation).

The energy functional based on the segmented MPS volume can be defined as

$$\begin{aligned} E(c_1,c_2,c_3,\Theta) &= \int_{D_1} |c_1 - G_\sigma * (J \circ T_\Theta)(x)|^2 dx \\ &+ \int_{D_2} |c_2 - G_\sigma * (J \circ T_\Theta)(x)|^2 dx \\ &+ \int_{D_3} |c_3 - G_\sigma * (J \circ T_\Theta)(x)|^2 dx \\ &= \int_\Omega \chi_{D_1}(x) \cdot |c_1 - G_\sigma * (J \circ T_\Theta)(x)|^2 dx \\ &+ \int_\Omega \chi_{D_2}(x) \cdot |c_2 - G_\sigma * (J \circ T_\Theta)(x)|^2 dx \\ &+ \int_\Omega \chi_{D_3}(x) \cdot |c_3 - G_\sigma * (J \circ T_\Theta)(x)|^2 dx, \end{aligned} \tag{1}$$

where c_1, c_2 and c_3 are constants that approximate the average intensities of regions D_1, D_2, and D_3, respectively, G_σ is a Gaussian kernel with standard deviation σ, and T_Θ is a rigid transformation of parameters $\Theta = (\theta_x, \theta_y, \theta_z, t_x, t_y, t_z)$ that denote rotations with respect to x, y and z directions and translations in x, y and z directions, respectively. The characteristic function χ_D is defined by

$$\chi_D(x) = \begin{cases} 1, & x \in D \\ 0, & x \notin D. \end{cases} \tag{2}$$

We apply a Gaussian filtering (with a standard deviation of 3mm) to the CTA volume to ensure homogeneous intensity levels, to suppress noise and to lower the CTA image resolution closer to that of the MPS image.

3.3. Minimization

The optimal values of parameters (c_1, c_2, c_3, Θ) to minimize the given energy functional are obtained by solving the associated Euler-Lagrange equations. As a numerical scheme, a gradient descent method is performed. The derivation of the Euler-Lagrange equations is given as below:

$$\frac{\partial \Theta_i}{\partial t} = -\frac{\partial E}{\partial \Theta_i} (i = 1, 2, \cdots, 6).$$

In the derivation, we consider only one term for a single region in the energy functional for simplicity, which is given by

$$\begin{aligned} -\frac{1}{2}\frac{\partial E}{\partial \Theta_i} = \int_\Omega \{\chi_D(x) \cdot (c - G_\sigma * (J \circ T_\Theta)(x))\} \\ \left(\frac{\partial}{\partial \Theta_i} (c - G_\sigma * (J \circ T_\Theta)(x) \right) dx \end{aligned} \tag{3}$$

By setting $T_\Theta(x) = T(\Theta, x)$, we get

$$\begin{aligned} &\frac{\partial}{\partial \Theta_i}(G_\sigma * (J \circ T_\Theta)(x)) \\ &= \int_{\mathbb{R}^2} G_\sigma(y) \frac{\partial}{\partial \Theta_i} \{J(T(\Theta, x-y))\} dy \\ &= \int_{\mathbb{R}^2} G_\sigma(y) \nabla J(T(\Theta, x-y)) \cdot \frac{\partial T(\Theta, x-y)}{\partial \Theta_i} dy. \end{aligned} \tag{4}$$

Furthermore, by setting $\frac{\partial J \circ T_\Theta(x)}{\partial \Theta_i} = L_i(\Theta, x) = \nabla J(T(\Theta, x)) \cdot \frac{\partial T(\Theta, x)}{\partial \Theta_i}$, we obtain

$$\begin{aligned} &\frac{\partial}{\partial \Theta_i}\left(G_\sigma * (J \circ T_\Theta)(x)\right) \\ &= \int_{\mathbb{R}^2} G_\sigma(y) L_i(\Theta, x-y) dy = G_\sigma * L_i(\Theta, x). \end{aligned} \tag{5}$$

Hence, Eq. (3) becomes

$$\begin{aligned} &-\frac{1}{2}\frac{\partial E}{\partial \Theta_i} \\ &= \int_\Omega \{\chi_D(x) \cdot (c - G_\sigma * (J \circ T_\Theta)(x))\} G_\sigma * L_i(\Theta, x) dx. \end{aligned} \tag{6}$$

By keeping Θ fixed, the minimization of the energy E with respect to constants c_1, c_2 and c_3 leads to

$$\begin{cases} c_1 = \dfrac{\int_\Omega \chi_{D_1}(x) \cdot (G_\sigma * (J \circ T_\Theta)(x))\, dx}{\int_\Omega \chi_{D_1}\, dx}, \\ c_2 = \dfrac{\int_\Omega \chi_{D_2}(x) \cdot (G_\sigma * (J \circ T_\Theta)(x))\, dx}{\int_\Omega \chi_{D_2}\, dx}, \\ c_3 = \dfrac{\int_\Omega \chi_{D_3}(x) \cdot (G_\sigma * (J \circ T_\Theta)(x))\, dx}{\int_\Omega \chi_{D_3}\, dx}. \end{cases} \tag{7}$$

The constant intensity values and transformation parameters can be minimized using Eqs. (6) and (7) in an alternative manner.

4. EXPERIMENTAL RESULTS

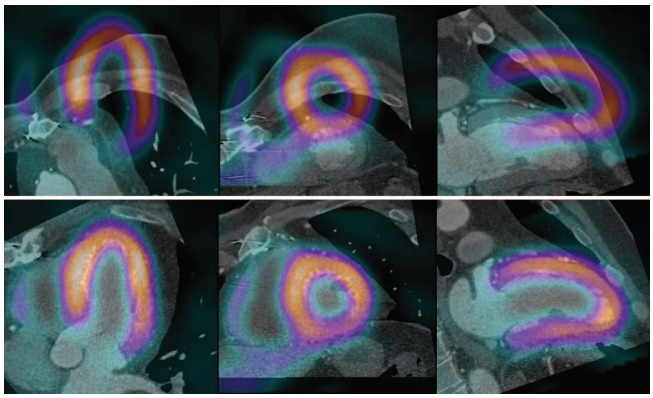

Fig. 3. An example of registration results: images before (top) and after (bottom) registration are shown. Errors were (1, 2, 1) mm for the translation and (2, 0, 0) degrees for the rotation in this case.

Registration results using the proposed method and a normalized mutual information (NMI) method have been compared with the manual alignment (n=40) obtained by two observers on 20 stress/rest MPS (64×64×24, 6.4×6.4×6.4mm) and CTA (512×512×260, 0.49×0.49×0.63mm) datasets acquired by two CT scanners (10 GE VCT 64-slice scanner and

10 Siemens 64-slice Dual Source CT scanner). An example of CTA and MPS pair and its registration result are shown in Fig. 3.

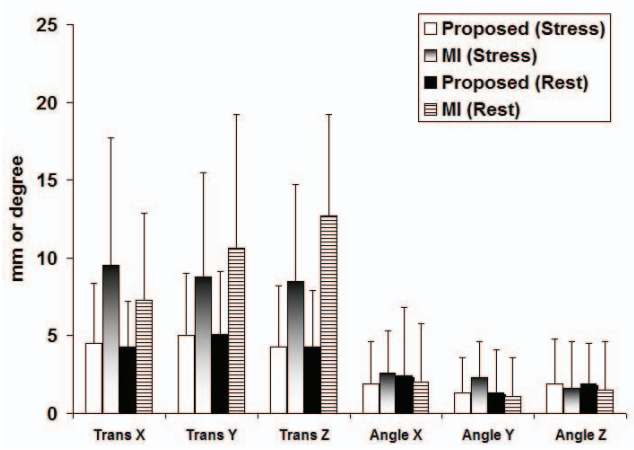

Fig. 4. Registration errors for stress and rest

Our registration of MPS with CTA achieved a success rate of 100% and the average registration time was 10±1.3 sec. The MI based registration method had a larger error than proposed one as shown in Fig. 4 and the average registration time was 24±2.2 sec. The translational and rotational registration results were not much different in inter-observer variability and in the stress and rest MPS (p=NS) as shown in Table 1. No significant difference between different types of scanners was observed. That is, 4.5±3.3 mm for translation and 1.2±2.1 degrees for rotation for Siemens and 4.6±3.5 mm for translation and 2.2±3.4 degrees for rotation for GE (p=NS).

The preliminary studies show that the proposed approach fulfills fast and accurate results with the registration accuracy of less than a MPS voxel size, which is feasible to be used for clinical practice.

Table 1. Registration error and observer variability

		translation (mm)	rotation (degree)
MI based Method	Stress	9.0±7.0	1.5±3.1
	Rest	10.2±7.3	1.5±1.6
Proposed Method	Stress	4.6±3.3	1.7±2.6
	Rest	4.5±3.1	1.8±3.1
Observer Variability	Stress	3.1±2.4	2.8±3.3
	Rest	3.7±2.9	2.6±3.8

5. CONCLUSION

A multi-modality registration algorithm of coronary CTA with MPS in a variational framework was presented. A segmentation algorithm for extracting the blood pool, myocardium, and extracardiac structures from MPS was adopted before registration. In the registration process, segmented regions in MPS were aligned to the corresponding regions in coronary CTA by utilizing geometrically characteristic features obtained by MPS segmentation and the homogeneity property of intensities within regions of interest in coronary CTA. It was demonstrated by experimental results that the proposed algorithm outperformed a standard registration method based on the normalized mutual information. The potential of the proposed algorithm in clinical applications for integrated MPS analysis to resolve borderline cases is enhanced by its computational efficiency.

6. REFERENCES

[1] S. Achenbach, "Cardiac ct: State of the art for the detection of coronary arterial stenosis," *Journal of Cardiovascular Computed Tomography*, vol. 1, no. 1, pp. 3–20, 2007.

[2] P. Viola and W. M. Wells, "Alignment by maximization of mutual information," *International Journal of Computer Vision*, vol. 24, no. 2, pp. 137–154, 1997.

[3] F. Maes, A. Collignon, D. Vandermeulen, and et al., "Multimodality image registration by maximization of mutual information," *IEEE Trans Med Imaging*, vol. 16, pp. 187–198, 1997.

[4] A. Yezzi, L. Zollei, and T. Kapur, "A variational framework for integrating segmentation and registration through active contours," *Medical Image Analysis*, vol. 7, no. 2, pp. 171–185, 2003.

[5] O. Gaemperli, T. Schepis, and et al., "Cardiac image fusion from stand-alone spect and ct: Clinical experience," *J Nucl Med*, vol. 48, no. 5, pp. 696–703, 2007.

[6] O. Gaemperli, T. Schepis, and et al., "Validation of a new cardiac image fusion software for three-dimensional integration of myocardial perfusion spect and stand-alone 64-slice ct angiography," *Eur J Nucl Med Mol Imaging*, vol. 34, no. 7, 2007.

[7] T. L. Faber, C. A. Santana, and et al., "Three-dimensional fusion of coronary arteries with myocardial perfusion distributions: Clinical validation," *J Nucl Med*, vol. 45, no. 5, 2004.

[8] C. Guetter, M. Wacker, C. Xu, and J. Hornegger, "Registration of cardiac spect/ct data through weighted intensity cooccurrence priors," *MICCAI, LNCS*, vol. 4791, 2007.

[9] U. E. Aladl, G. A. Hurwitz, D. Dey, and et al., "Automated image registration of gated cardiac single-photon emission computed tomography and magnetic resonance imaging," *J Magn Reson Imaging*, vol. 19, no. 3, pp. 283–90, 2004.

[10] G. Germano, H. Kiat, P. B. Kavanagh, and et al., "Automatic quantification of ejection fraction from gated myocardial perfusion spect," *J Nucl Med*, vol. 36, no. 11, pp. 2138–47, 1995.

[11] P. J. Slomka, H. Nishina, D. S. Berman, and et al., ""motion-frozen" display and quantification of myocardial perfusion," *J Nucl Med*, vol. 45, pp. 1128–34, 2004.

[12] F.L. Bookstein, "Principal warps: Thin-plate splines and the decomposition of deformations," *IEEE Transactions on Pattern Analysis and Machine Intelligence*, vol. 11, no. 6, 1989.